LBL-24892 c.2

Lawrence Berkeley Laboratory
UNIVERSITY OF CALIFORNIA

APPLIED SCIENCE DIVISION

RECEIVED
LAWRENCE
BERKELEY LABORATORY

JUN 23 1988

LIBRARY AND
DOCUMENTS SECTION

Presented at the Third International Conference on Carbonaceous Particles in the Atmosphere, Berkeley, CA, October 5–8, 1987

A Concurrent-Flow Cloud Chamber Study of Incorporation of Black Carbon into Droplets

W.H. Benner, A.D.A. Hansen, and T. Novakov

April 1988

TWO-WEEK LOAN COPY

This is a Library Circulating Copy which may be borrowed for two weeks.

APPLIED SCIENCE DIVISION

LBL-24892 c.2

Prepared for the U.S. Department of Energy under Contract Number DE-AC03-76SF00098.

DISCLAIMER

This document was prepared as an account of work sponsored by the United States Government. While this document is believed to contain correct information, neither the United States Government nor any agency thereof, nor the Regents of the University of California, nor any of their employees, makes any warranty, express or implied, or assumes any legal responsibility for the accuracy, completeness, or usefulness of any information, apparatus, product, or process disclosed, or represents that its use would not infringe privately owned rights. Reference herein to any specific commercial product, process, or service by its trade name, trademark, manufacturer, or otherwise, does not necessarily constitute or imply its endorsement, recommendation, or favoring by the United States Government or any agency thereof, or the Regents of the University of California. The views and opinions of authors expressed herein do not necessarily state or reflect those of the United States Government or any agency thereof or the Regents of the University of California.

A CONCURRENT-FLOW CLOUD CHAMBER STUDY OF INCORPORATION OF BLACK CARBON INTO DROPLETS*

W.H. Benner, A.D.A. Hansen, and T. Novakov

Applied Science Division
Lawrence Berkeley Laboratory
University of California
Berkeley, California 94720

Abstract

A concurrent-flow cloud chamber (16 cm i.d., 1.5 m high) is described in which cold particle-free and humidified particle-laden air streams were mixed to condense water droplets onto combustion-generated soot particles. Total and interstitial black carbon (BC) concentrations in the cloud were measured as a function of input black carbon concentration and the sample air stream dew point in real time, using a two-channel aethalometer. For black carbon particles produced by the combustion of propane, as much as 90% (by mass) of the black carbon when [BC] < 5 $\mu g/m^3$ was incorporated; this decreased to ~ 20% when [BC] > 20 $\mu g/m^3$. It was observed that as sample dew point passed through a maximum, simultaneous maxima were observed in the fraction of black carbon incorporated into droplets and in the amount of black carbon associated with large droplets that settled out of the air stream. The effective supersaturation in the chamber is a function of particle concentration. For black carbon particle concentrations above ~ 20 $\mu g/m^3$, the estimated supersaturation is of the order of several percent for the experimental conditions used.

*This work was supported by the Director, Office of Energy Research, Office of Health and Environmental Research, Physical and Technological Research Division of the U.S. Department of Energy under Contract No. DE-AC03-76SF00098 and by the National Science Foundation under Contract No. ATM-8713712.

Introduction

Combustion-generated soot particles play an important role in the atmosphere, mainly because of their light-absorbing and surface chemical properties. Soot particles also serve as a unique tracer for combustion-generated pollutants. The transport, concentration, distribution, and effects of soot particles are influenced by their water nucleation properties. The condensation of water vapor on aerosol particles and their phoretic, diffusive, or inertial capture by droplets may lead to the incorporation of particles into the aqueous phase and subsequently to their removal from the atmosphere by precipitation. These processes critically influence the residence time of the particles in the atmosphere. Soot particles that are effective cloud condensation nuclei will therefore have shorter atmospheric lifetimes than those unaffected by nucleation.

Dry soot particles may directly affect the atmospheric heat balance because of their unique light-absorbing properties. It has been suggested that incorporation of black carbon particles into cloud droplets may increase their optical absorptivity and thus change the albedo of the cloud (Chylek et al., 1984). Soot particles capable of nucleating cloud droplets may also influence the cloud albedo indirectly by modifying the size distribution of cloud droplets. Such aerosol-induced changes of the cloud microstructure may also alter the colloidal stability of clouds and fogs.

Because of these effects, it is important to know more about the nucleation properties of various types of soot and to understand which specific physical and chemical factors determine these properties. Most of the studies on the nucleation and scavenging properties of aerosols dealt with sulfates and nitrates and were motivated by the acid precipitation problem (Pruppacher et al., 1983). So far, however, very little emphasis has been on nucleation scavenging of soil particles, trace metals, and carbonaceous particles. Quite recently a few studies on the nucleation properties of soot have been reported in the context of the "nuclear winter" phenomenon (Hallett et al., 1987; Hagen et al., 1987). These studies have shown that wood smoke particles are much more active cloud condensation nuclei than particles from the combustion of clean jet aviation fuel (JP-4). These differences can be attributed to the differences in

chemical composition of the fuels, such as the ash content, and the surface chemical modification of particles during smoke formation. It has also been reported (Benner et al., 1987) that soot particles produced by combustion of the same fuel (propane) but with varying sulfur content have different nucleation characteristics. This effect is related to the flame oxidation of the fuel sulfur to SO_3, which may end up on a particle surface as a layer of hygroscopic sulfuric acid or sulfate.

The prevalent approach to the studies of nucleation properties of aerosols involves various thermal gradient or expansion chambers that operate at preselected supersaturation ratios. At high supersaturations (> 100%), all particles became condensation nuclei (CN). At low supersaturations of a few percent, usually only a fraction of the total particles, called cloud condensation nuclei (CCN), are activated. In the troposphere, water supersaturations are thought to be limited to < 1%. Thermal gradient or expansion chambers provide data on the particle number but not on the mass fraction of the activated aerosols and do not provide an easy way to determine the chemical composition of the activated and unactivated fractions of the aerosol because of the low concentrations of the particles that must be sampled. CN and CCN instruments use low concentrations because they employ single particle detection, and because of the requirement that the supersaturation ratio be determined solely by the temperature and humidity fields and not by droplet formation.

We have constructed a concurrent-flow cloud chamber, designed specifically for laboratory cloud chemistry and physics studies involving combustion products. The chamber design allows collection of adequately loaded filter samples of the unprocessed and the cloud-processed total and interstitial aerosol for subsequent chemical analyses, and provides for a quasi-real-time determination of black carbon in these aerosol fractions. This paper describes the chamber and its application to the measurement of nucleation properties and scavenging of soot particles.

Experimental

The cloud chamber, shown in Fig. 1, consists of a double-walled glass cylinder (16 cm i.d., 1.5 m tall). The sample air is drawn axially into the bottom of the chamber where it mixes with an annular flow

of filtered cold air to produce a rising and expanding cone of cloud droplets. Exit flow and input flow of cold air are adjusted so that exit flow exceeds cold flow. Internal surfaces of the system are of glass, Teflon, or aluminum.

This chamber is conceptually similar to a continuous cloud condensation nucleus counter originally developed by Langer (See Rosinski et al., 1984). The temperature and humidity fields resulting from the turbulent mixing of the two air flows determine the initial supersaturation of the water vapor. In the single particle applications of the Langer chamber, calculated supersaturations were about 2%. In our applications, however, the effective supersaturations also depend on the particle concentration. As the air mixture becomes supersaturated, an increasing number of particles will reach the unstable growth regime, rapidly remove the water vapor from the system, and reduce the supersaturation to less than that expected for the mixing of particle-free air streams.

The cloud chamber was connected to a combustor, which serves as the source of soot particles. In the combustor, propane (S < 10 ppm) was burned (111 ml/min) in a diffusion flame. The air was supplied to the flame by an annular flow (50 l/min) of filtered dilution air. Subsequent dilution of the combustion effluent allowed the concentration of soot in the cloud chamber to be maintained in the concentration range between 0.1 and 100 $\mu g/m^3$.

The temperature of the sample stream was maintained at 50°C, and its dew point controlled at a temperature between 40°C and 50°C. Depending on the flow rates of cold air, sample air, particle concentration, and sample dew point, clouds can be produced that vary from a very light cloud that was barely perceptible visually along a He—Ne laser beam to a very dense cloud that visually obscured objects at greater than 0.5 m. The sample dew point was adjusted by introducing humidified air flow into the sample stream. The humidification system consisted of a temperature-controlled water bubbler. To prevent the condensation of water on the inside of the inlet tubing, the sample inlet tubing, including the dew point particle filter, dew point sensor (chilled mirror type, General Eastern, Model 1200AP), and humidifier were maintained in a constant temperature (50°C) chamber. Because part of the sample inlet tubing

extends through the low-temperature region of the cold air inlet, this section was additionally heated to maintain its temperature at 50°C. The cold dilution air was dried by passage through silica gel and then cooled by passage through a heat exchanger. This heat exchanger was chilled by IPA that had been cooled to dry ice temperature in a second heat exchanger. The cold air introduced into the chamber could be adjusted between room temperature and -40°C; for the experiments described, it was maintained at -13°C ±2°C.

Temperatures throughout the system (Fig. 1) were measured with calibrated thermistors and monitored by a computer. The temperature of the sample air stream and humidifier were computer controlled to ±0.2°C of set temperature. Typical operating parameters (exhaust flow = 14.5 l/min; cold air flow = 10.5 l/min, T = -13°C; particle-laden "sample" flow = 1.2 l/min; humidified air flow = 2.8 l/min, T = 50°C, dew point = 47°C) produced a cloud at room temperature (20 ± 2°C); therefore the chamber jacket temperature was controlled by equilibrium with room temperature. With these operating conditions, the resulting chamber air mixture temperature and liquid water content (LWC) were calculated to be T_{mix} = 0.4°C and LWC = 11.4 g/m^3. In actuality, the mixture temperature was ~ 18°C due to heat that is conducted into the chamber. This addition of heat, with respect to the calculations, is equivalent to having a cold air temperature of 10°C. Thus for T_{mix} = 18°C and a cold air temperature of 10°C, the cloud is calculated to contain 0.2 g/m^3 LWC. These operating conditions allowed a small amount of water vapor to condense on the lower part of the chamber wall, but this amount of condensation had a negligible influence on cloud formation.

Air samples could be withdrawn from the top of the chamber through three tubes. One tube was used as a bypass flow when the sampling equipment was being connected or disconnected from the other two tubes. The second sampling tube was heated to evaporate cloud droplets and therefore sampled the total (interstitial and occluded) aerosol. The third tube was preceded by a droplet-separating mesh (Brewer et al., 1983) (three layers of mesh, 102-μm diameter fibers, 96% void volume; Kimre, Inc., Perrine, Fla.). At the 7.25 l/min sampling flow rate, factory-supplied data indicated that collection efficiency

was greater than 90% for droplets larger than 6 μm in diameter but minimal for the interstitial aerosol. Liquid water collected by the mesh accumulated on the downstream side (upper surface when positioned vertically) and could easily be removed by low-speed centrifugation for subsequent chemical analysis and liquid water content determinations. The difference in concentrations of particles in the total and interstitial sampling tubes equals the concentration of particles incorporated in droplets.

Total and interstitial black carbon concentrations were monitored with a two-channel aethalometer. The aethalometer, described previously (Hansen et al., 1984), measures in real time the transmission of white light through ~ 1 cm diameter particle deposits collected on a quartz fiber filter. The aethalometer response is converted to BC concentration by the specific attenuation (Gundel et al., 1984) of black carbon.

Results and Discussion

In this section we will first present data pertaining to the performance and stability of the experimental system, and then describe our results on propane soot nucleation as a function of chamber operating conditions. Because of the specifics of the chamber design, precise flow control is required. For example, with 14.5 l/min exhaust flow rate, 10.5 l/min cold air input, and 2.8 l/min humidified flow, the resulting sample input rate is 1.2 l/min. If particle concentrations in the chamber were to be maintained within ±10%, then the exhaust flow rate had to be controlled at ±1%. The flow rate stability in the chamber is illustrated in Fig. 2. The chamber [BC] concentration of 0.94 ±.05 $\mu g/m^3$ (x ± s.d.) was successfully maintained over a 75-min period. This 5% variation in concentration is about as good as can be expected for the present design and the flow rates used. At higher concentrations good stability was also observed. Occasionally, greater concentration variations were observed that could be attributed to fluctuations in the soot yield of the flame.

Dew point of the sample flow as a function of time was recorded for each experiment. Figure 3 is an example of the achievable dew point stability during a 4-hr period. During two equilibrated operating conditions (0—100 and 140—240 min), the dew point was controlled at 43°C ±.5°C and 45°C ±0.8°C,

respectively. After increasing the humidifier temperature at 100 min, the sample dew point equilibrated at the higher level after about 30 min.

The stability of the aethalometer operating system is shown in Fig. 4, where the concentration ratios of $[BC]_I/[BC]_T$ in the two aethalometer channels in the absence of cloud was plotted vs. time. $[BC]_I$ is the BC concentration following the mesh separator and corresponds to the interstitial black carbon concentration and $[BC]_T$ is the total (interstitial + droplet) black carbon concentration. This ratio being equal to (1.0 ±.01) shows that with no cloud in the chamber, the mesh did not collect a measurable fraction of the black carbon particles. The black carbon concentration in the chamber was varied between 4 and 6 $\mu g/m^3$ in this experiment.

The effect of sample air dew point on the cloud formation and the incorporation of soot particles into droplets is shown in Fig. 5a and b. Fig. 5a shows the variation of the dew point as a function of time, and Fig. 5b, represents the concentrations of total and interstitial black carbon at the top of the chamber. Initially, total concentration was ≈ 7 $\mu g/m^3$. With the sample dew point of 28.9°C, no cloud was visible in the chamber. In the absence of cloud, the ratio of interstitial to total black carbon was equal to one. The sample dew point was gradually increased to 44.4°C and then decreased to 38.3°C. During this dew point cycle, the fraction of black carbon incorporated into droplets started at zero and increased to 0.78 before returning to zero again. Maximum incorporation was observed when the dew point of the particle-laden air stream increased from 41.2°C to 44.4°C.

From the data shown in Fig. 5, it can be seen that the total black carbon concentration reaching the top of the chamber decreases during the time of maximum incorporation and maximum dew point, even though the concentration in the inlet stream was held constant. A tentative explanation of this observation is that some of the soot-containing droplets grow to large sizes, whose sedimentation velocities exceed the upward velocity of air in the chamber, and thus are removed by gravitational settling. For this to happen, droplets would need to grow in excess of ~ 20 μm diameter. Other more complex scavenging processes may also take place, however. From Fig. 5 we can estimate that 10% of the initial black car-

bon remained as interstitial particles, 45% was incorporated into droplets, and 45% was removed by other scavenging processes in the chamber.

The mass fraction of black carbon incorporated into cloud droplets, for constant chamber conditions, depends on the input concentrations. This is shown in Fig. 6, where the percent of incorporation is plotted as a function of total black carbon concentration for a 46.7°C dew point sample stream. At concentrations < 5 $\mu g/m^3$, ~ 90% of the carbon was incorporated into droplets. This percentage decreased nearly linearly as the concentration was increased to 17 $\mu g/m^3$. Above 17 $\mu g/m^3$ the percentage remains essentially constant. For a constant water vapor input, a fixed amount of water vapor is available for droplet formation in the chamber, which has to be distributed among the active nuclei. The maximum saturation ratio in a cloud is determined by a balance between the droplet growth rate and the decrease in saturation vapor pressure that occurs when vapor condenses (Penner and Edwards, 1986). Both these processes, growth of larger droplets and diffusionally limited growth, cause a larger fraction of particles to be detected in droplets when the black carbon concentration is relatively small, as shown in Fig. 6. The cloud chamber at low particle concentrations operates at a regime similar to that in a CN counter, while at higher concentrations it resembles conditions in a CCN chamber.

In the experiments described here, the actual supersaturation ratio was not determined. However, changes in sample dew point can be expected to cause changes in the supersaturation ratio. We can estimate that the effective supersaturation ratio for moderately high particle concentrations (20—100 $\mu g/m^3$) is in the range of a few percent. This estimate is based on the comparison of the results obtained with our chamber for wood and JP-4 jet fuel smoke with those of Hallett et al. (1987). They measured the ratios of cloud condensation nuclei to total condensation nuclei for the same two fuels and reported that the number fractions for particles incorporated into droplets were 0.7 and 0.01 for wood and JP-4 respectively. The experiments in our chamber with an average sample dew point of 45.6°C have shown that 42% and 9% by mass of the wood and JP-4 soot respectively are incorporated into droplets at input concentrations of 20—50 $\mu g/m^3$. These percentages were 30% and 3% respectively for input concentrations

between 50 and 100 $\mu g/m^3$. The reasonable agreement between the two sets of results suggest that at particle concentrations above ~ 20 $\mu g/m^2$, the effective supersaturation in the chamber is in the cloud condensation range of approximately a few percent.

References

Benner, W.H., Hansen, A.D.A., and Novakov, T. (1987). In *Applied Science Division Annual Report*, Lawrence Berkeley Laboratory Report LBL-22150, p. 4-7.

R.L. Brewer, R.J. Gordon, and L.S. Shepard. (1983). *Atmos. Environ.* 17:2267-2270.

P. Chylek, W. Ramaswamy, and V. Srivastava. (1984). *Sci. Total Environ.* 36:117-120.

L.A. Gundel et al. (1984). *Sci. Total Environ.* 36:197-202.

D.E. Hagen, M.B. Trueblood, and D.R. White. (1987). [Paper presented at Third International Conference on Carbonaceous Particles in the Atmosphere, Oct. 5-8, 1987, Berkeley, California; this volume.]

J. Hallett, J.G. Hudson, and C.F. Rogers. (1987). [Paper presented at Third International Conference on Carbonaceous Particles in the Atmosphere, Oct. 5-8, 1987, Berkeley, California; this volume.]

A.D.A. Hansen, H. Rosen, and T. Novakov. (1984). *Sci. Total Environ.* 36:191-196.

Penner, J.E., and Edwards, L.L. (1986) Lawrence Livermore National Laboratory report UCRL-93800.

Pruppacher, H.R., Semonin, R.G., and Slinn, W.G.N., editors. (1983). *Precipitation, Scavenging, Dry Deposition, and Resuspension, Vol. 1: Proceedings of the Fourth International Conference on Precipitation Scavenging.* Elsevier, New York.

J. Rosinski et al. (1984). *J. Aerosol Sci.* 15:709-715.

Figure Captions

Figure 1 Schematic diagram of the cloud chamber.

Figure 2 Demonstration of the achievable black carbon concentration stability in the chamber.

Figure 3 Long-term dew point stability of the inlet particle-laden air stream. The humidifier temperature was increased at 100 min .

Figure 4 Demonstration of the aethalometer channel stability for constant input black carbon concentration in the absence of cloud. $[BC]_I$ and $[BC]_T$ are the concentrations in the interstitial and total channels.

Figure 5 (a) A cycle in the dew point of the inlet particle-laden air stream that produced changes in the incorporation of BC into droplets as shown in (b). Lightly hashed histogram bars represent $[BC]_T$ and darker hashed bars represent $[BC]_I$.

Figure 6 The effect of $[BC]_T$ on the fractional incorporation of BC into droplets.

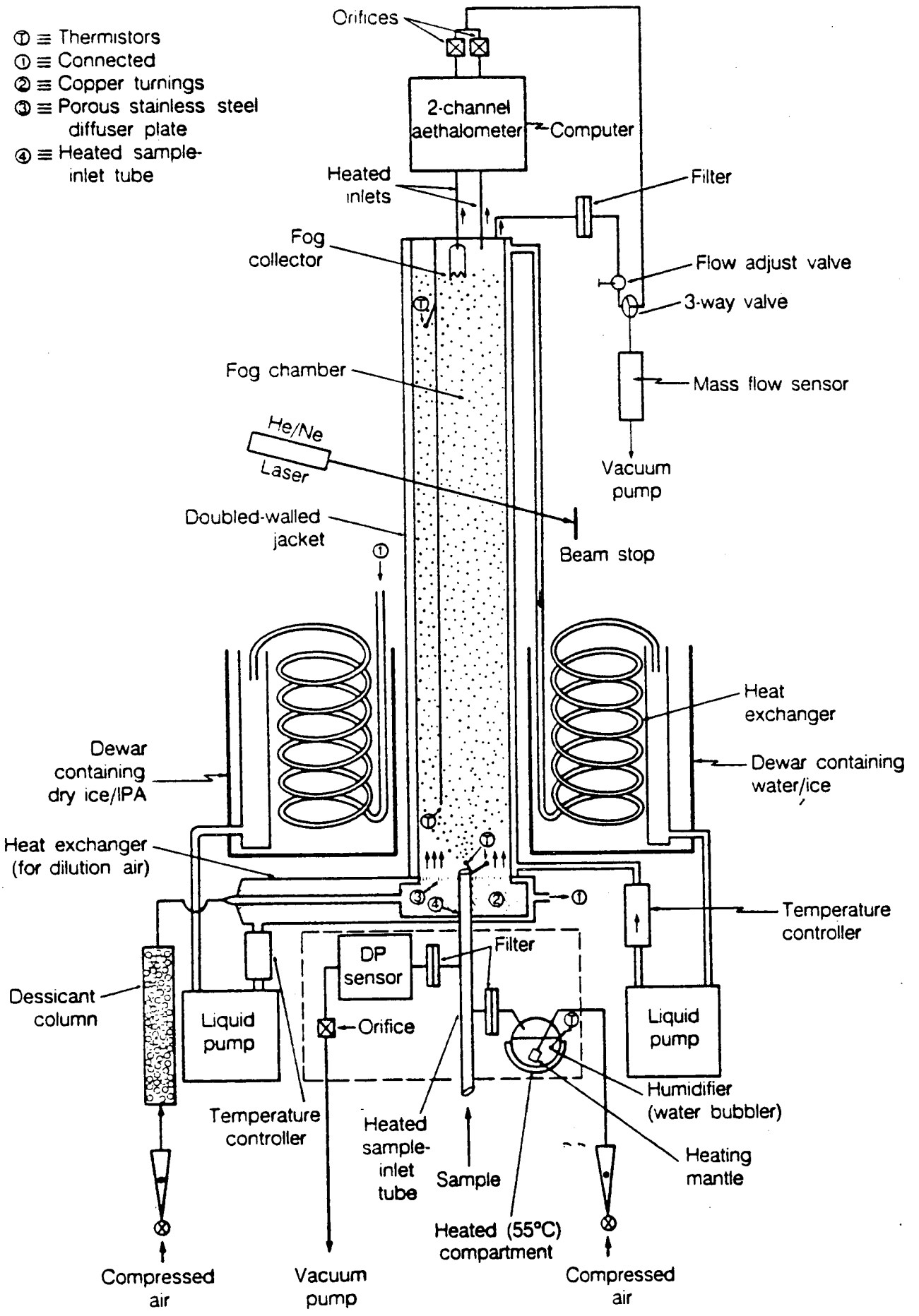

Figure 1

-- XBL 873-1128 --

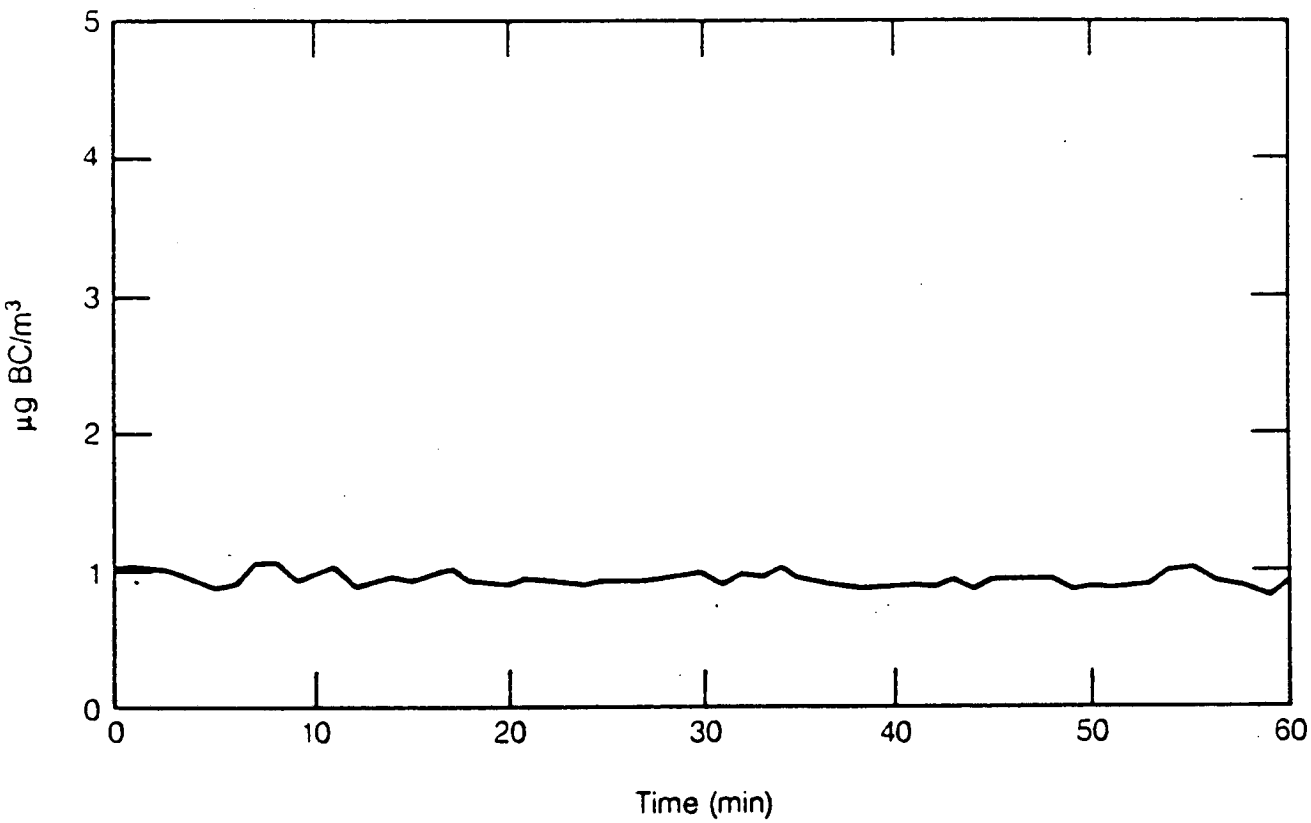

XBL 879-3803A

Figure 2

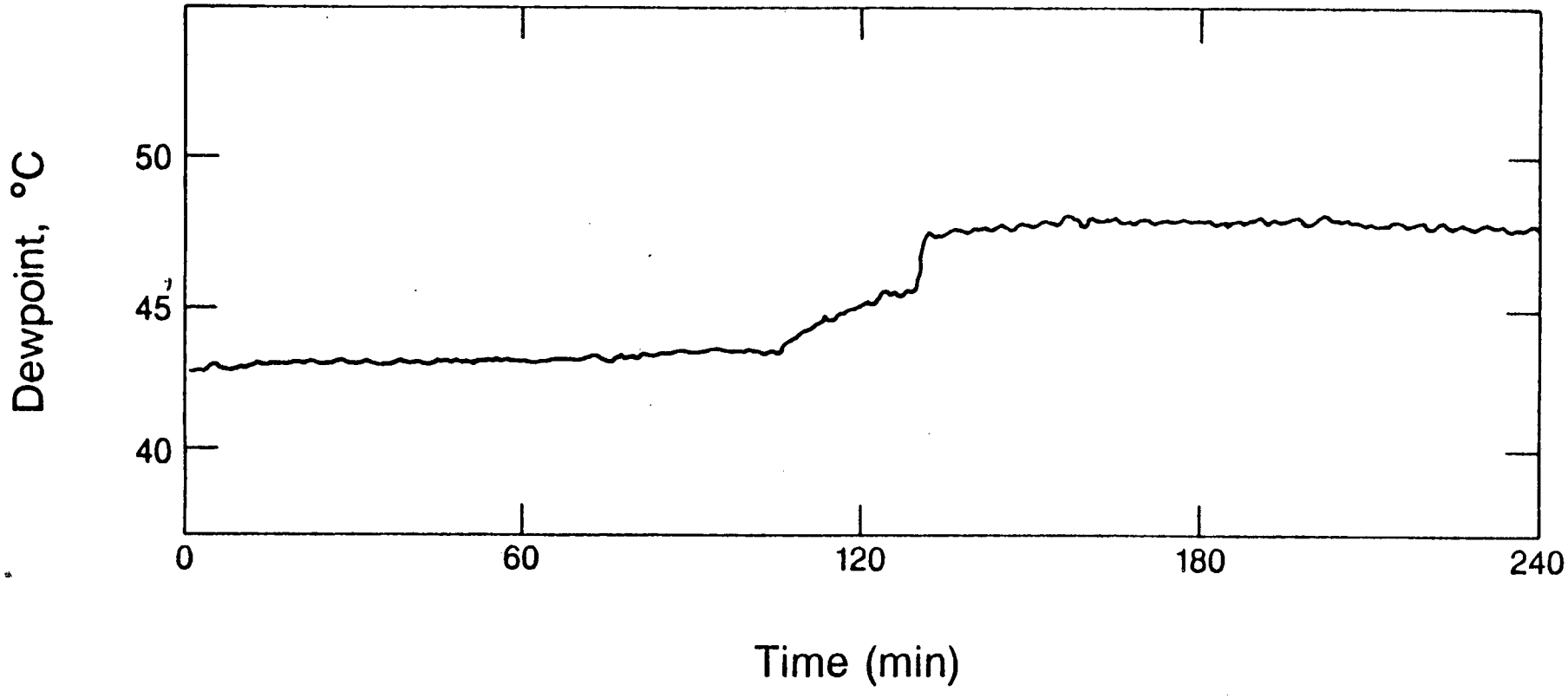

Figure 3

XBL 878-9755A

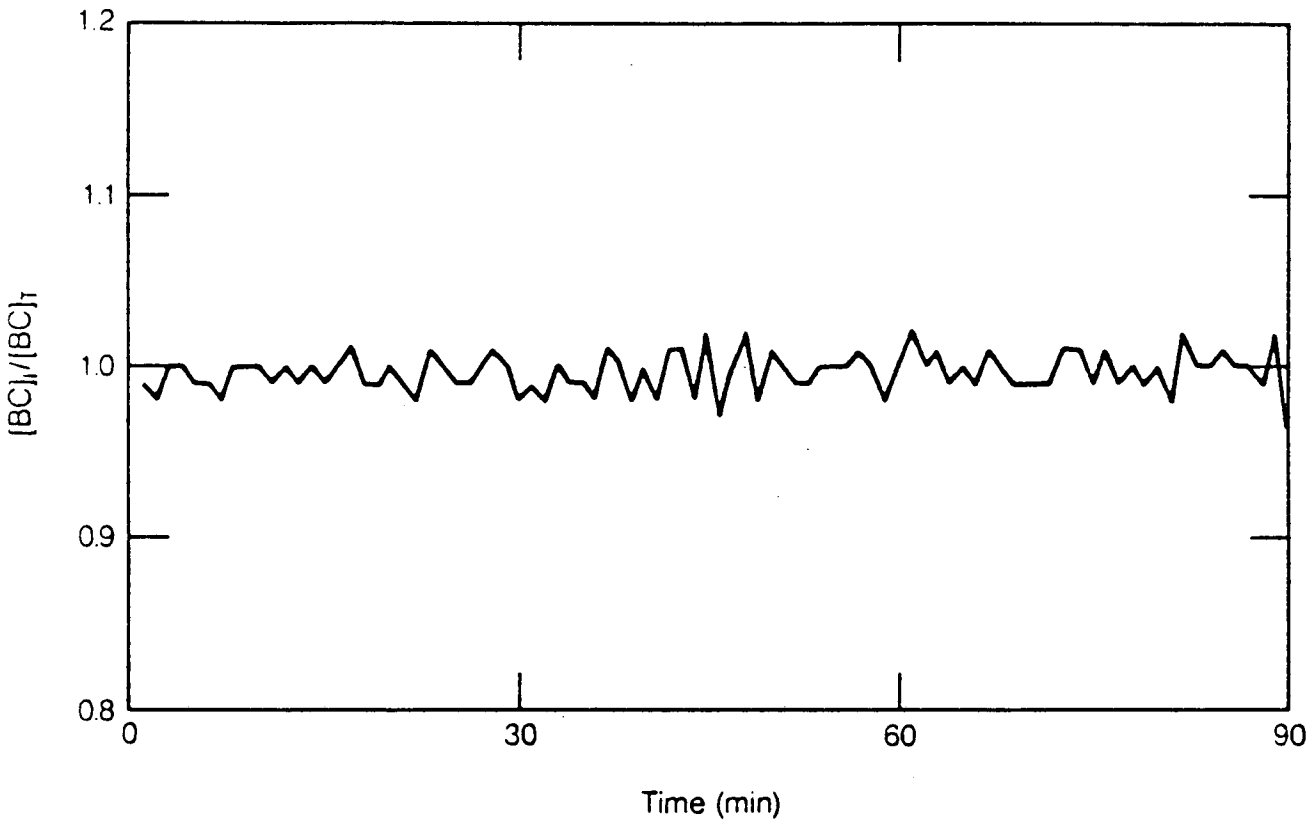

XBL 879-3804A

Figure 4

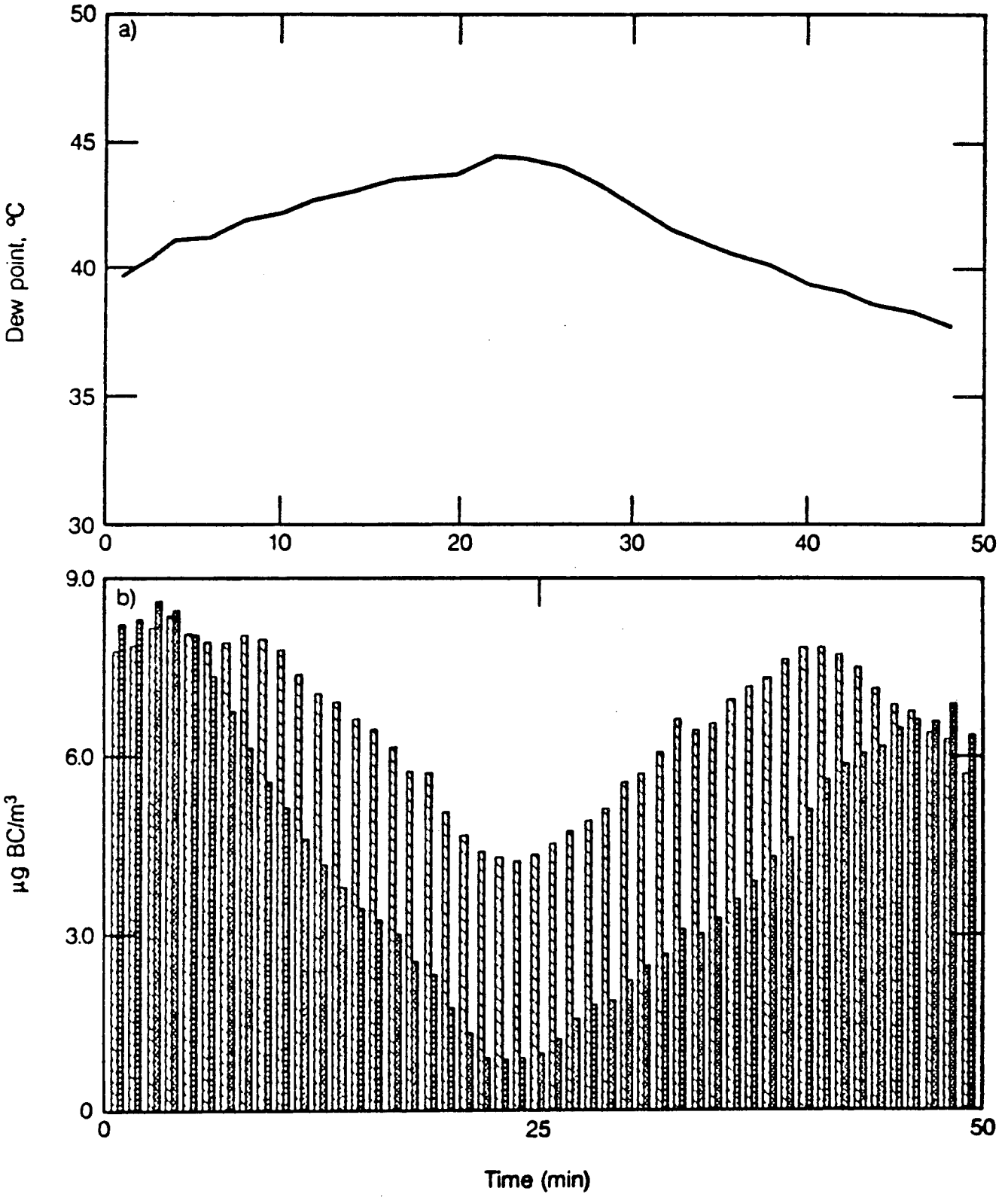

Figure 5

XBL 879-3805A

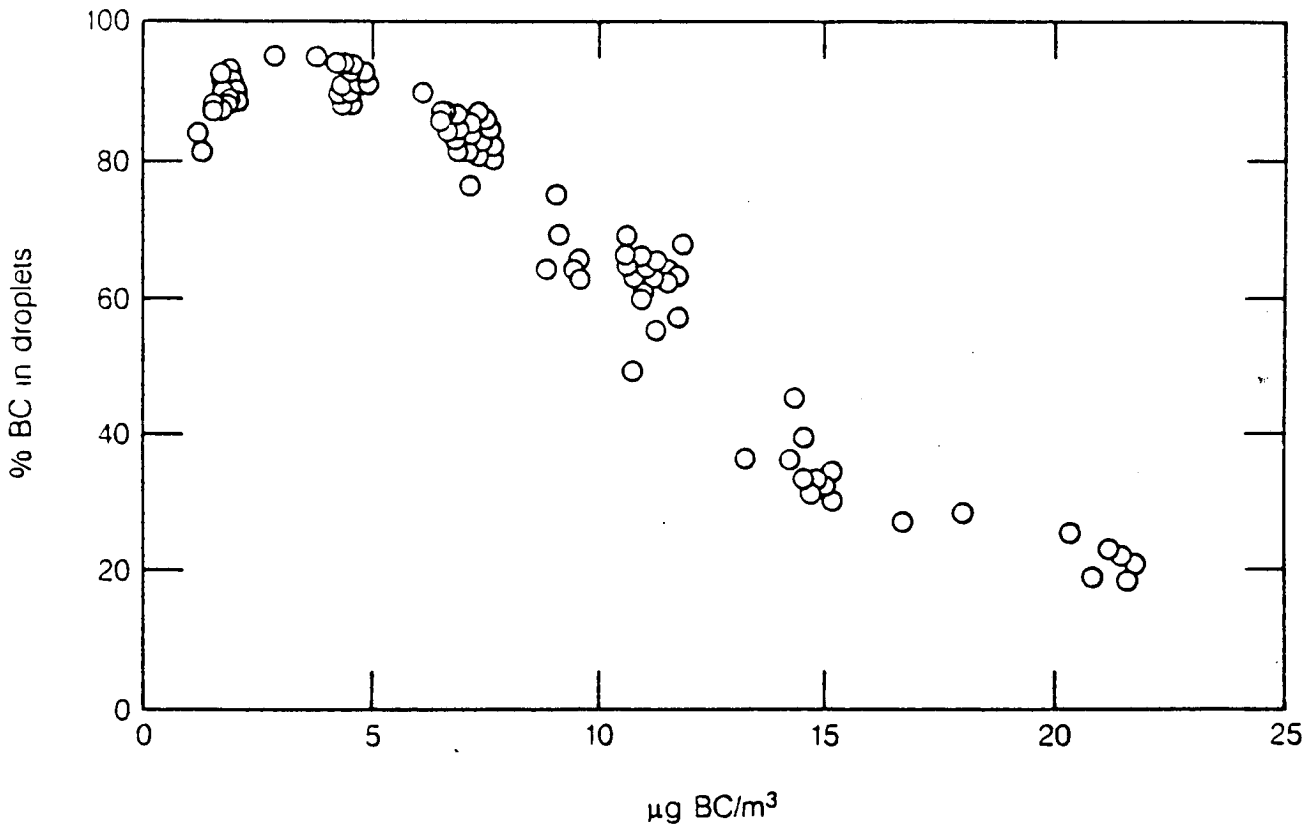

Figure 6

XBL 873-720A

LAWRENCE BERKELEY LABORATORY
TECHNICAL INFORMATION DEPARTMENT
UNIVERSITY OF CALIFORNIA
BERKELEY, CALIFORNIA 94720